Journal of Materials and Electronic Devices 5 (2021) 1-6

DFT based calculations of Acid Molecules on 2D C_3N nanosheets: QTAIM, NCI Analysis

S. SENTURK DALGIC[1] and F. KANDEMIRLI[2]

[1]Trakya University, Department of Physics, Edirne, Turkey
[2]Kastamonu University, Department of Biomedical Engineering, Kastamonu, TURKEY

In this work, we have first presented the density functional theory (DFT) based calculations, such as Quantum Theory of Atoms in Molecules (QTAIM) and Non-covalent interaction (NCI) analysis for the interactions of organic acid molecules of phosphoric acid (H_3PO_4) and sulphuric acid (H_2SO_4) molecules with two dimensional (2D)-polyaniline (C_3N) nanosheet. Thus, the most stable geometries, adsorption properties and the nature of interactions of acid molecules on 2D-C_3N have obtained. The density functional theory (DFT) calculations were carried out with GAUSSIAN program package. Our results reveal that 2D-C_3N nanosheet is a promising adsorbent for phosphoric acid as E_{ads} of H_3PO_4/ C_3N complex is -20 kcal/mol whereas for H_2SO_4/ C_3N complex is about -7,78 kcal/mol in the gas phase. Although, the QTAIM and NCI results indicate that there is strong interaction between H_3PO_4 molecule and C_3N nanosheet as partially covalent character, the weak interaction between H_2SO_4 molecule and C_3N nanosheet is obtained. Furthermore, 2D-C_3N nanosheet is less sensitive to both H_3PO_4 and H_2SO_4 molecules. While a reasonable recovery time is obtained for H_3PO_4 molecule about 160,57 sec., this time is very short for sulphuric acid molecule. The presented atomic structure of 2D-C_3N surface may use an organic surface where phosphoric acid and sulphuric acid molecules can be easily cleaned.

Keywords: *2D-PANI, 2D-C_3N, Bronsted acid molecules, DFT, QTAIM, GAUSSIAN*

Submission Date: 05 May 2021
Acceptance Date: 01 September 2021

**Corresponding author: serapd@trakya.edu.tr , dserap@yahoo.com*

1. Introduction

Recently, two dimensional (2D) materials have attracted great attention in many fields due to their unique chemical and physical properties [1-3]. 2D materials have the thin thickness and large surface to volume ratio, thus their electronic and magnetic properties can be tuned by the adsorption of molecules. After graphene discovery, researchers started to find the new 2D materials, which is analogous to graphene. On the other hand, theoretical studies have been predicted carbon-nitrogen C-N compounds such as CN, C_3N, C_3N_2, etc. It has been found that the carbon-based structure with stoichiometry C3N has a layered structure containing graphitic layers **.** Thus, it has reported 2D PANI with empirical formula as C_3N added to two-dimensional carbon family. The C_3N is a semiconductor which is useful for many applications in solar cell devices, doping of transistors, anode material. Theoretical calculations showed that the electronic properties of 2D-PANI can be tuned in different ways. Recently, the sensing ability of C_3N surfaces for toxic volatile organic compounds such as ethanol, methanol, isopropanol and isobutanol molecules has been first reported [3]. In our previous work, melting process of gold nanoparticles on 2D-PANI

nanosheets was investigated by molecular dynamics simulations [4]. According to our knowledge,

there is a few studies on Bronsted acid molecules on graphene sheets [5]. However, there is no a comprehensive knowledge about the adsorption of acid molecules on 2D-PANI (2D-C_3N) surfaces.
The adsorption properties of organic acid molecules on 2D-C_3N nanosheet has been first reported in this work.

2. Materials and Method

In order to obtain a deeper knowledge on the interactions between the selected organic acid molecules on 2D-C_3N surfaces, density functional theory (DFT) calculations has been carried out. All calculations were done using the Gaussian 09 package [6]. The results reported in this work were obtained with DFT calculations at the B3LYP/6-311G (d,p) level. The 2D-C_3N nanosheet is created with hexagonal primitive unit cell. The planar hexagonal nanosheet of C_3N include 32 atoms. The optimized structures of 2D-C_3N nanosheet, organic molecules used in this work are shown in Fig. 1.

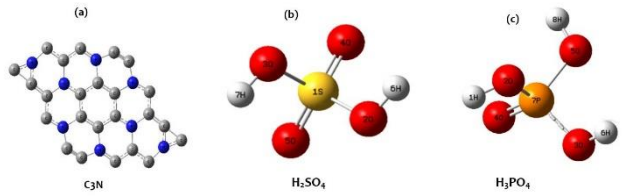

Fig.1. Optimized structures of (a) C_3N (b) H_2SO_4 (c) H_3PO_4 molecule. *Here, carbon, nitrogen, hydrogen, oxygen, phosphor and sulphur are represented by grey, blue, white, red, orange and yellow spheres, respectively.*

Adsorption energies of acid molecules on 2D-C_3N nanosheet E_{ads} were computed as follows:

$$E_{ads}(\text{molecule}) = E(complex) - E(2D{-}C_3N) - E(molecule) \quad (1)$$

where $E(\text{complex})$, $E(2D - C_3N)$ and $E(\text{molecule})$ are the total energies of the 2D-C3N/acid molecule as denoted complex and isolated energies of 2D-C_3N Nanosheet and studied acid molecules, respectively.
Chemical stability was mainly influenced by the highest occupied molecular orbital (HOMO) and the lowest unoccupied molecular orbital (LUMO), where the (HOMO) and the (LUMO) can play an important role in electrical properties. The LUMO represents electron-accepting, while the HOMO represents electron-donating ability. The HOMO and LUMO energies give a lot of essential quantities. Band gap energy can be expressed as:

$$\Delta E_g = E_{LUMO} - E_{HOMO} \quad (2)$$

Recovery Time:

An important parameter for sensors is the recovery time (τ) which can be described as follows:

$$\tau = \upsilon^{-1} exp\left(-\frac{E_{ads}}{kT}\right) \quad (3)$$

where υ is the attempt frequency, for UV vacuum light ($\upsilon \sim 10^{12}\ sn^{-1}$) , k is the Boltzmann constant and T is temperature.
Recovery time gives the time required for the material to be desorbed from the adsorbents. This parameter is exponentially related to the adsorption energy, so their weak interaction results in a small amount of adsorption energy and a small desorption.
In order to understand the nature of bonding between acid molecules on 2D-C_3N nanosheet, the quantum theory of atoms in molecules (QTAIM) based on Bader's theory [7] was performed by MULTIWFN program [8]. The topological parameters, the electron density of bonding regions were analysed in optimized geometries of complexes. The second tool of analysing of molecular interactions is non-covalent interactions (NCI) analysis based on reduced gradient density (RDG). The NCI/RDG analysis was carried out by MULTIWFN code [8]. The coloured maps of scatter points and isosurfaces of RDG were plotted by gnuplot 5.7 program [9] and visual molecular dynamics (VMD1.9.4) package [10], respectively.

3. Results and Discussions

The hexagonal 2D-C_3N nanosheet was considered as an adsorbent of acid molecules. First, each acid molecules and 2D-C_3N were optimized separately using DFT calculation in gas phase. In order to investigate stable geometries, we have tried different positions of acid molecules on 2D-C_3N nanosheet. The preferable adsorption geometries have been found as complex 1 and complex 2 structures for H_3PO_4 and complex 3 structure for H_2SO_4 molecule on 2D-C_3N nanosheet. The results for those structures have been given in Table 1. The calculated adsorption energy of E_{ads}, dipole moment μ, HOMO and LUMO energies and band gap energy ΔEg values have been shown in Table1.

Table 1. The calculated E_{ads} adsorption energy, μ dipole moment, HOMO and LUMO energies E_{LUMO}, E_{HOMO} and band gap energy ΔEg values for the studied structures.

Structure.	E_{ads} (kcal/mol)	μ (Debye)	E_{HOMO} (eV)	E_{LUMO} (eV)	ΔE_g (eV)
2D-C_3N	-	1.262	-6.425	-5.220	1.205
H_3PO_4	-	3.459	-8.433	-0.137	8.295
H_2SO_4	-	3.276	-9.391	-0.443	8.949
complex 1 H3PO4/2D-C_3N	-17.053	2.792	-6.308	-5.048	1.260
complex 2 H3PO4/2D-C_3N	-20.049	4.150	-6.567	-5.359	1.209
complex 3 H_2SO_4/ 2D-C_3N	-7.7822	5.912	-6.150	-4.890	1.261

It is clear in table 1 that the 2D-C_3N nanosheet is a good adsorbent for H_3PO_4 molecule than H_2SO_4. The H_3PO_4 molecule was adsorbed on the 2D-C_3N nanosheet with the adsorption energy about -17.053 kcal/mol for complex 1 and -20.049 kcal/mol for complex 2 at a minimum distance of about 1.84, 3.07 and 2.00, 1.92Å. The H_2SO_4 molecule was adsorbed on the 2D-C_3N nanosheet with the adsorption energy about -7.7822 kcal/mol for complex 3 at a minimum distance of about 3.16, 3.18Å.

In table 1, the energy gap of 2D-C_3N increases from 1.205eV to 1.260 eV for complex 1, 1.209 eV for complex 2 and 1.261 eV for complex 3 after the interaction with H_3PO_4 and H_2SO_4, acid molecules, respectively. It has pointed out that the $\%\Delta E_g$ which is the percentage change of energy gap of E_g after adsorption with respect to the bare C_3N nanosheet, for complex 2, is about 0.33 % and for complex 3 is 4.45 %. It is correlated with the level of interactions such as strong or weakly thus the adsorption energy and charge transfer during the adsorption process.

On this line, Mulliken charge analysis was performed to obtain the charging values of 2D-C_3N nanosheet $Q_{2D\text{-}C3N}(e)$ during the adsorption process of acid molecules. It has been found that the charge transfers from 2D-C_3N nanosheet to phosphoric acid molecule of H_3PO_4 in complex 2, about $Q_{2D\text{-}C3N}$ (in complex 2) =0,0658e. However, the charge transfer is from acid molecule to 2D-C_3N nanosheet in complex 3, with the value of $Q_{2D\text{-}C3N}$ (in complex 3) = -0,0282e.

Quantum Theory of Atoms in Molecules (QTAIM) Analysis

The QTAIM method is a power tool for studying the nature of intermolecular interactions and structure of bonds. According to this theory, the critical point of electron density can be classified the following four categories as *Atomic* critical point (ACP); bond critical point (BCP); ring critical point (RCP); and cage critical point (CCP). The computed molecular topographical map of both complex 2 and complex 3 with critical points is illustrated in Fig. 2.

In QTAIM analysis, mostly, the electron density of $\rho(r)$ and laplacian $\nabla^2\rho(r)$ characteristics are widely used to understand the bonding interactions nature. However, the total energy density of H(r) and the ratio of $|V(r)|/G(r)$ are more remarkable parameters on bonding characteristics. It has been noted that for weak and medium-strength hydrogen bonding and van der Waals interactions due to the $\nabla^2\rho(r) > 0, H(r) > 0, |V(r)|/G(r) < 1$, for covalent bonding characteristics correspond to $\nabla^2\rho(r) < 0, H(r) < 0, |V(r)|/G(r) > 2$. The strong hydrogen bonds as the intermediate type of interaction related to $\nabla^2\rho(r) > 0, H(r) < 0, 1 < |V(r)|/G(r) < 2$.

The QTAIM parameters for complex 2 and complex 3, electron density ρ_{BCP}, Laplacian $\nabla^2\rho_{BCP}$, potential, kinetic and total energy density (V_{BCP}, G_{BCP} and H_{BCP}) in a.u, Bond distance (Å), $|V_{BCP}|/G_{BCP}$ ratio, at BCPs are given in Table 2.

Table 2. The QTAIM parameters of the selected complexes at the BCPs.

Structure	BCPs	ρ_{BCP}	$\nabla^2\rho_{BCP}$	G_{BCP}	V_{BCP}	H_{BCP}	$\|V_{BCP}\|/G_{BCP}$
Complex2 H_3PO_4/C_3N	H38-C5	0.0326351	0.065516	0.01910238	-0.0218257	-0.0027233	1,142561
	O36-C5	0.0135446	0.0405839	0.91939E-02	-0.00824183	0.0095207	0,896445
	H40-C18	0.0367638	0.0639552	0.020748402	-0.02550799	-0.0047595	1,229395
Complex3 H_2SO_4/C_3N	O36-C14	0.0065834	0.0238698	0.004969531	-0.00397162	0.0009979	0,799194
	O37-C11	0.0063649	0.0231674	0.004805271	-0.00381869	0.0009865	0,794687

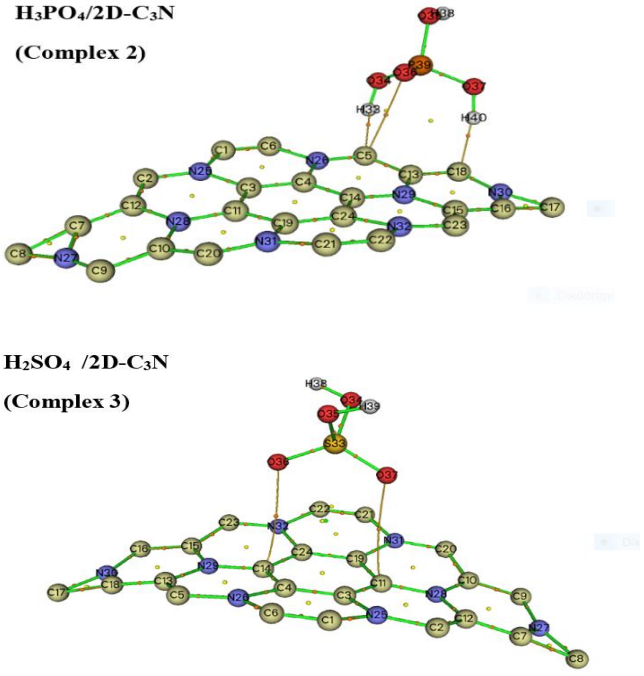

Fig. 2. Molecular topography map for complex 2 and complex 3

In Fig 2, atomic and bond critical points are presented by purple and orange spheres, respectively. The cage and ring critical points due to green and yellow circles.

The topology map for complex 2 in Fig. 2 shows that the Bond critical Points are between the hydrogen atoms of H38 and H40 of phosphoric acid molecules and carbon atoms of C5 and C18 of 2D-C3N nanosheet, respectively. Other bonding can be observed between oxygen atom of acid molecule and C5 atom of C_3N surface. In the molecular topography map for Complex 3, the two bonding is observed between oxygen atoms of sulphuric acid molecules and carbon atoms of nanosheet.

The QTAIM results in Table2 give information about the bonding characteristics. The last column values about the ratio of v(r) /g(r) are 1,142561 and 1,229395 for H38-C5 and H40-C18 interactions in complex 2, respectively due to the medium-strength hydrogen bonding. That means those interactions are strong and partially covalent character. However, the interaction corresponds to O36-C5 is a weak interaction like van der Waals type. For complex 3 both interactions are nearly weak and wander Waals type character. Thus, we can apply non-covalent interaction (NCI) analysis to find any other type of interactions.

Non-Covalent Interaction (NCI)- Reduced Gradient Density (RDG) Analysis

NCI analysis method can be regarded as an extension of the QTAIM theory for visual study. RDG analysis is able to find noncovalent interactions which is determined through the sign of the second density Hessian eigenvalue of λ_2.

The interactions can be defined as attractive if $(sign\,\lambda 2)\,\rho < 0$ (namely, strong attraction) and weak van der Waals interaction if $(sign\,\lambda 2)\,\rho \approx 0$, and strong repulsive interactions if $(sign\,\lambda 2)\,\rho > 0$ and (steric effect in ring). The plot of RDG versus (sign λ2) ρ(r) and RDG isosurface map for complex 2 and complex 3 are shown in Fig. 3. And Fig.4, respectively.

In Figs 3 and 4, RDG scatter plots and isosurface maps for complex 2 and complex 3 are visualized the interactions by different colours. The strong interactions in partially covalent character between H and C atoms as shown by blue circles in Fig. 3b correspond to cross sign placed at blue region part of Fig. 3a. The weak interactions are shown by green circle between O and C atoms in Figure 3b correspond to cross sign pointed out in Fig. 3a.

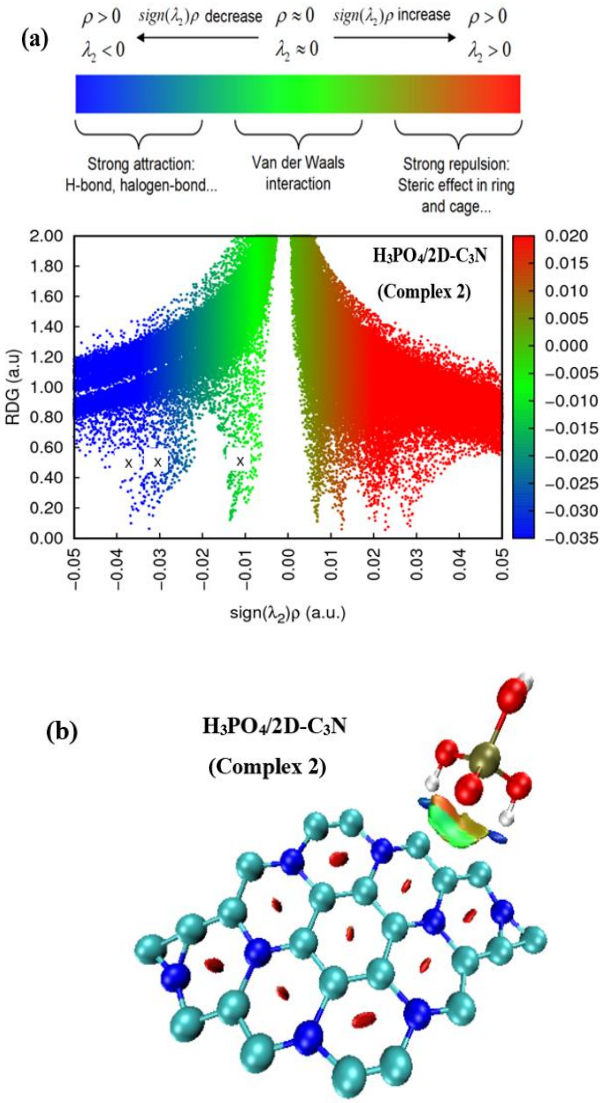

Fig. 3. (a) RDG scatter plot and (b) RDG isosurface map for complex 2

The RDG scatter plots and isosurface map are shown for complex 3 in Fig. 4 where we observe the weak interactions in partially van der Waals type between Oxygen and C atoms of phenyl ring as shown by green circles in Fig. 4b correspond to cross sign placed at green region part in Fig. 4a. The third interaction cannot be seen in QTAIM Figures of Fig.2. Because it is rather weak and between the sulphur and carbon atoms. The weak interactions are shown by green circle in Fig. 4b

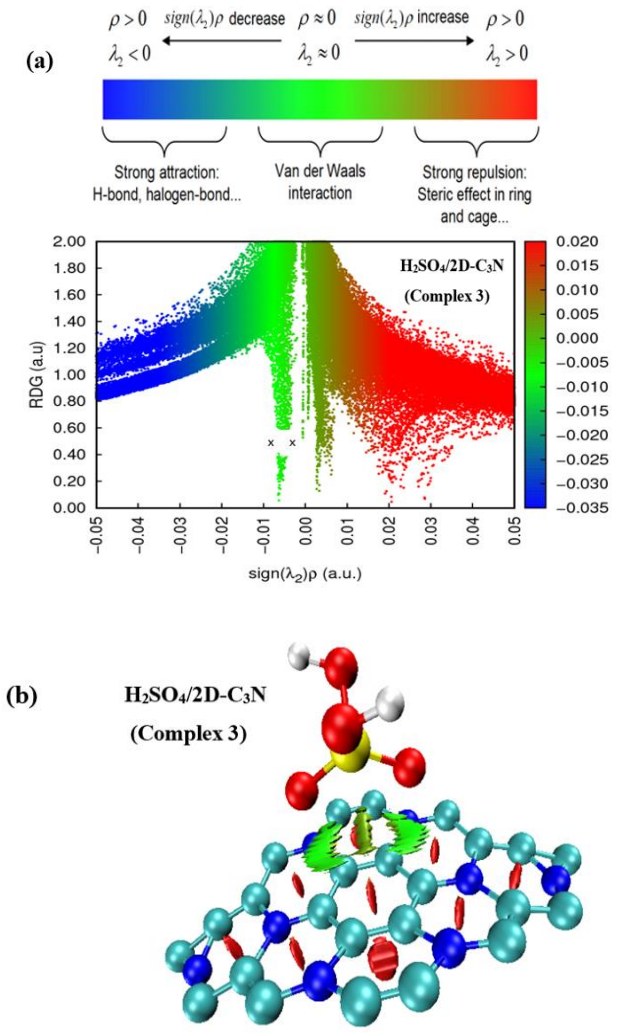

Fig. 4. (a) RDG scatter plot and (b) RDG isosurface map for complex 3

The recovery time is calculated under UV vacuum light at room temperature for complex 2 and complex 3 as given in Table 3. Those values are the time values in second to recover of acid molecules from the 2D-C_3N nanosheet.

Table 3. Recovery time (τ) values for complex 2 and complex 3

Complex	$\tau^{UV\ vacuum\ light}$(sec)
H_3PO_4/2D-C_3N complex 2	160,57
H_2SO_4/2D-C_3N complex 3	1.66 x 10^{-7}

The recovery time of H_2SO_4 molecule is very short time to desorb from 2D-C_3N surfaces. However, the desorption time obtained for H_3PO_4 molecule is a reasonable value about 160,57 sec.

4. Conclusion

In this study, DFT calculations are performed to understand the adsorption behaviours of organic acid molecules of H_3PO_4 and H_2SO_4 on new generation organic nanosheet of C_3N. obtained. The exothermic adsorption process was determined for both H_3PO_4 and H_2SO_4 acid molecules with the negative adsorption energy values about -17.053, -20.049, -7.7822 kcal/mol in the gas phase for complex 1, complex 2 and complex 3, respectively.

The closest distances show that H_3PO_4 adsorption through hydrogen atoms with carbon atoms of nanosheet is thermodynamically more favourable than interaction from oxygen site at both positions of complex 1 and complex 2.

The percentage change of band gap values show that 2D-C_3N nanosheet has less sensing performance in detecting both acid molecules. Therefore, 2D-C_3N nanosheet doesn't suit for potential applications as both H_3PO_4 and H_2SO_4 sensor in studied configurations. The calculated Recovery Time value for H_2SO_4 molecule is too short to desorb of H_2SO_4 molecule from 2D-C_3N surfaces at room temperature. However, the value of 160sec is a reasonable recovery time for H_3PO_4.

We conclude that the presented atomic structure of 2D-C_3N surface may have a great attention to use an organic surface where phosphoric acid and sulphuric acid molecules can be easily cleaned.

And we hope that the current theoretical work may play an important role in guiding related experimental researches.

References

[1] H. Zhang, Ultrathin Two-Dimensional Nanomaterials ACS Nano 9 (2015) 9451-9469

[2] B. Liu, K. Zhou, "Recent progress on graphene-analogous 2D nanomaterials: Properties, modelling and applications", Progress in Materials Science, 100 (2019) 99-169.

[3] S. Agrawal, G. Kaushal and A. Sirvastava, Electron transport in C_3N monolayer: DFT analysis of volatile organic compound sensing, Chemical Physics Letters, 762 (2021) 138121.

[4] S. Senturk Dalgic, 2D PANI/GOLD Nanocomposites: A Molecular Dynamics Study, Proceedings of 4th International Organic Electronic Material Technology Conference (OEMT 2019), 1-5

[5] N. I. Kovtyukhova, Y. Wang, A. Berkdemir, R. Cruz-Silva, M. Terrones, V.H. Cresp and T. E. Mallouk, Non-oxidative intercalation and exfoliation of graphite by Bronsted acids, Nature chemistry, 6 (2014) 957-963.

[6] Frisch, M. J.; Trucks G. W.; Schlegel, H. B.; Scuseria, G. E.; Robb, M. A.; Cheeseman, J. R.; Scalmani, G.; Barone, V.; Mennucci, B.; Petersson, G. A.; Nakatsuji, H.; Caricato, M.; Li, X.; Hratchian, H. P.; Izmaylov, A. F.; Bloino, J.; Zheng, G.; Sonnenberg, J. L.; Hada, M.; Ehara, M.; Toyota, K.; Fukuda, R.; Hasegawa, J.; Ishida, M.; Nakajima, T.; Honda, Y.; Kitao, O.; Nakai, H.; Vreven, T.; Montgomery, J. A.; Peralta, J. E.; Ogliaro, F.; Bearpark, M.; Heyd, J. J.; Brothers, E.; Kudin, K. N.; Staroverov, V. N.; Kobayashi, R.; Normand, J.; Raghavachari, K.; Rendell, A.; Burant, J. C.; Iyengar, S. S.; Tomasi, J.; Cossi, M.; Rega, N.; Millam, J. M.; Klene, M.; Knox, J. E.; Cross, J. B.; Bakken, V.; Adamo, C.; Jaramillo, J.; Gomperts, R.; Stratmann, R. E.; Yazyev, O.; A. J. Austin, A. J.; Cammi, R.; Pomelli, C.; Ochterski, J. W.; Martin, R. L.; Morokuma, K.; Zakrzewski, V. G; Voth, G. A.; Salvador, P.; Dannenberg, J. J.; Dapprich, S.; Daniels, A. D.; Farkas, O.; Foresman, J. B.; Ortiz, J. V.; Cioslowski, J.; Fox, D. J. Gaussian, Inc. , Gaussian 09, Revision D.01, Wallingford CT, 2013.

[7] Bader R.F.W., Atoms in molecules, Acc. Chem. Res. 18 (1985) 9–15.

[8] Lu T., F. Chen, Multiwfn: a multifunctional wave function analyser, J. Comput. Chem. 33 (2012) 580–592.

[9] W. Thomas, C. Kelley, 1 gnuplot (2004).

[10] Humphrey, W.; Dalke, A.; Schulten, K. VMD: Visual Molecular Dynamics. J. Mol. Graphics 1996, 33−38.